Poly(ether imide)s Containing Cyano Substituents and Thin Films Made from Them

Irina Bacosca,[1] Elena Hamciuc,[1] Mariana Cristea,[1] Gabriela Lisa,[2] Maria Bruma[1]

[1]*"Petru Poni" Institute of Macromolecular Chemistry, Aleea Gr. Ghica Voda 41A, Iasi 700487, Romania*
[2]*"Gh. Asachi" Technical University, Faculty of Chemical Engineering and Environmental Protection,*
B-dul D. Mageron 71, Iasi 700050, Romania

Received 24 November 2010; accepted 15 May 2011
DOI 10.1002/app.34914

ABSTRACT: A series of poly(ether imide)s containing functional cyano groups has been prepared by polycondensation reaction of 2,6-bis(*m*-aminophenoxy)benzonitrile with different bis(ether dianhydride)s, such as 2,2-bis[4-(3,4-dicarboxyphenoxy)phenyl]isopropane dianhydride, 2,2-bis[4-(3,4-dicarboxyphenoxy)-phenyl]hexafluoroisopropane dianhydride, 1,1-bis[4-(3,4-dicarboxyphenoxy)phenyl] cyclohexane dianhydride, and 3,3-bis[4-(3,4-dicarboxyphenoxy) phenyl]phthalide dianhydride. The polymers were soluble in polar aprotic solvents and even in less polar solvents and were processed into thin films by casting their solutions. The properties of the polymers, particularly the crosslinking of macromolecular chains through cyano groups, were studied by using dynamic mechanical analysis (DMA), thermal stability, glass transition, and solubility measurements. Also, the molecular relaxations were evidenced by DMA and dielectric spectroscopy. © 2011 Wiley Periodicals, Inc. J Appl Polym Sci 124: 1956–1966, 2012

Key words: polyimides; thin films; thermal properties; crosslinking

INTRODUCTION

The efforts to discover new structures with high thermal stability and good processability are focused on heterocyclic polymers. The best results were obtained on polyimides.[1] Aromatic polyethers are also a class of high performance polymers which draw attention because of their easy processability, good resistance to solvents, and excellent mechanical properties.

The incorporation of heterocycles into the chains of aromatic polyethers leads to the increase of glass transition temperature and of elastic modulus. Such an example is poly(ether imide) Ultem 1000 obtained and commercialized by General Electric (Fairfield, Conneticut, United States), which is easily processable, has high thermal stability and good mechanical properties. The aim to obtain a good thermostability maintaining in the same time processability can be achieved by preparing aromatic poly(ether imide)s with asimetric aromatic units substituted in *ortho* or *meta* position. Other heterocycles introduced in the macromolecular chains of polyethers to obtain enhanced properties are 1,3,4-oxadiazole, phenylquinoxaline, triazole, oxazole, benzoxazole, benzimidazole, pyrimidine, triazine, tiantrene, and benzoilenbenzimidazole.[2,3]

Poly(ether imide)s are thermostable heterocyclic polymers which contain imide cycles and ether linkages along the macromolecular chains. The synthesis can be performed by substitution aromatic nucleophylic reactions with the formation of ether linkage or by cyclodehydration reactions with the generation of imide cycle using adequate monomers: diamines and dianhydrides with ether bonding.[4]

Thermostable resins have an excellent combination of high thermal stability, chemical and flame resistance due to the networks formed in the crosslinking process. Such polymers are used as base materials for high resistant adhesives, coatings, or composite materials in a variaty of applications. It is known that a good approach to obtain curable polymers is the introduction of curable styril, nitrile, and phenyl groups into the macromolecular chains. The curing of nitrile-containing polymers can be done in the absence of catalysts, without evolution of volatiles.[5–7] The nitrile group is easily introduced into the polymer chains in pendant or terminal position and can be transformed through trimerization in *s*-triazine rings, which offer an excellent thermal stability and an increased adhesion to many substrates.[8–10] The resulting thermosetting polymers can be used in applications which require high thermo-oxidative and high performance structural properties at elevated temperatures.[11]

Correspondence to: I. Bacosca (ibacosca@icmpp.ro).

Contract grant sponsor: CNCSIS-UEFISCDI, project code PNII-IDEI; contract grant number: ID_997/2008.

Journal of Applied Polymer Science, Vol. 124, 1956–1966 (2012)

Recently, much research has been made on the synthesis and characterization of polyimides containing pendent nitrile polar groups, especially with the aim to develop new high temperature piezoelectric materials for sensor and actuator fabrication.[12–14] On our knowledge, only a few data are reported concerning poly(ether imide)s containing cyano groups.[15] This article presents the synthesis and characterization of new poly(ether imide)s containing functional cyano groups based on the reaction of 2,6-bis(*m*-aminophenoxy)benzonitrile with a series of bis(ether anhydride)s, and the study of thin films made from such polymers.

EXPERIMENTAL

Measurements

Melting points of the monomers and intermediates were measured on a Melt-Temp II (Laboratory Devices).

Elemental analysis was performed with a CHNS 2400 II Perkin Elmer instrument.

Infrared spectra were recorded on a FT-IR Bruker Vertex 70 analyzer, by using KBr pellets or polymer films.

^{1}H-NMR (400 MHz) spectra were obtained on a Bruker Avance DRX 400 spectrometer. The polymer samples were dissolved in DMSO-d_6 on heating and then measured at room temperature or were dissolved in a mixture of solvents ($CDCl_3$: CF_3COOD = 9/1, v/v) at room temperature.

Model molecules for a polymer fragment were obtained by molecular mechanics (MM+) by means of the Hyperchem program, Version 7.5.[16] The calculation were carried out with full geometry optimization (bond lengths, bond angles and dihedral angles).

The inherent viscosities of the polymers were determined at 20°C, by using NMP-polymer solutions of 0.5 g dL^{-1} concentration, with an Ubbelohde viscometer.

Average-molecular weights were measured by means of gel permeation chromatography using a PL-EMD 950 evaporative mass detector instrument. Polystyrene standards of known molecular weight were used for calibration and tetrahydrofurane as the mobile phase.

Wide angle X-ray diffraction (WAXD) was performed on a Bruker D8 ADVANCE Difractometer, using the Ni-filtered Cu-Ka radiation (λ = 0.1541 nm). A MRI-WRTC–temperature chamber (with nitrogen inert atmosphere) and a MRITCPU1-temperature control and power unit were used. The working conditions were 36 kV and 30 mA. All the diffractograms were investigated in the range 1.5–40° (2θ degrees), at different temperatures. Initial samples for X-ray measurements were powders obtained directly by polycondensation. All diffractograms are reported as observed.

The quality of the films was investigated by atomic force microscopy (AFM). The images were taken in air, on a SPM SOLVER Pro-M instrument.

The glass transition temperature (T_g) was measured on a Mettler DSC 12E apparatus in nitrogen with a heating rate of 20°C min^{-1}. The mid-point of the inflection curve resulting from the typical second heating cycle was considered as the T_g of polymers.

The thermogravimetric study was performed under constant nitrogen flow (20 mL min^{-1}) at heating rates: 7, 10, 13, and 16°C min^{-1} using a Mettler Toledo TGA/SDTA 851 balance. The heating scans were performed on 2 to 4 mg of sample in the temperature range 25–900°C. The thermal and kinetic characteristics of the polymers were analyzed with STAR program and "Kinetics *n*th order" modulus, respectively.

Dynamic mechanical analysis (DMA) was performed with a Perkin Elmer Diamond apparatus equipped with a standard tension attachment. The experiments were run on film samples with dimensions 10 × 10 × 0.04 mm by heating from 0°C up to beyond the temperature of the glass transition, with a heating rate of 2°C min^{-1}. The film samples were longitudinally deformed by a small sinusoidal stress at a frequency of 1 Hz, and the resulting strain was measured. The variations of the storage modulus E', loss modulus E'', and tension loss tangent tan d (tan $d = E''/E'$) as functions of temperature were obtained.

Dielectric spectroscopy (DEA) measurements of the polymer films at various temperatures in the range of −150–300°C and in the frequency range of 10^{-1}–10^6 Hz have been performed using a Novocontrol Dielectric Spectrometer (GmbH, Germany), CONCEPT 40. Polymer films were placed in a flat parallel plate capacitor arrangement having gold-plated electrodes with 20 mm diameter. The thickness of the films was in the range of 0.04–0.07 mm. The amplitude of AC applied voltage was 1 V.

Synthesis of monomers and polymers

2,6-Bis(*m*-aminophenoxy)benzonitrile (**1**) was synthesized by the reaction of nucleofilic substitution of 2,6-diclorobenzonitrile with *m*-aminophenol;[17,18] m.p.**1** = 136–138°C.

Bis(ether anhydride)s (**2**) were synthesized by a multistep reaction, according to the literature.[19–22] In the first step, 4-nitrophtalonitril reacts with different aromatic diols containing isopropylidene, hexafluoroisopropylidene, phthalide, or cyclohexane units, in dimethylformamide as solvent and in the presence of potassium carbonate. In the second step, the resulting tetranitrile is hydrolyzed to the corresponding tetracarboxylic acid; the final step is the dehydration of that tetracarboxylic acid by using

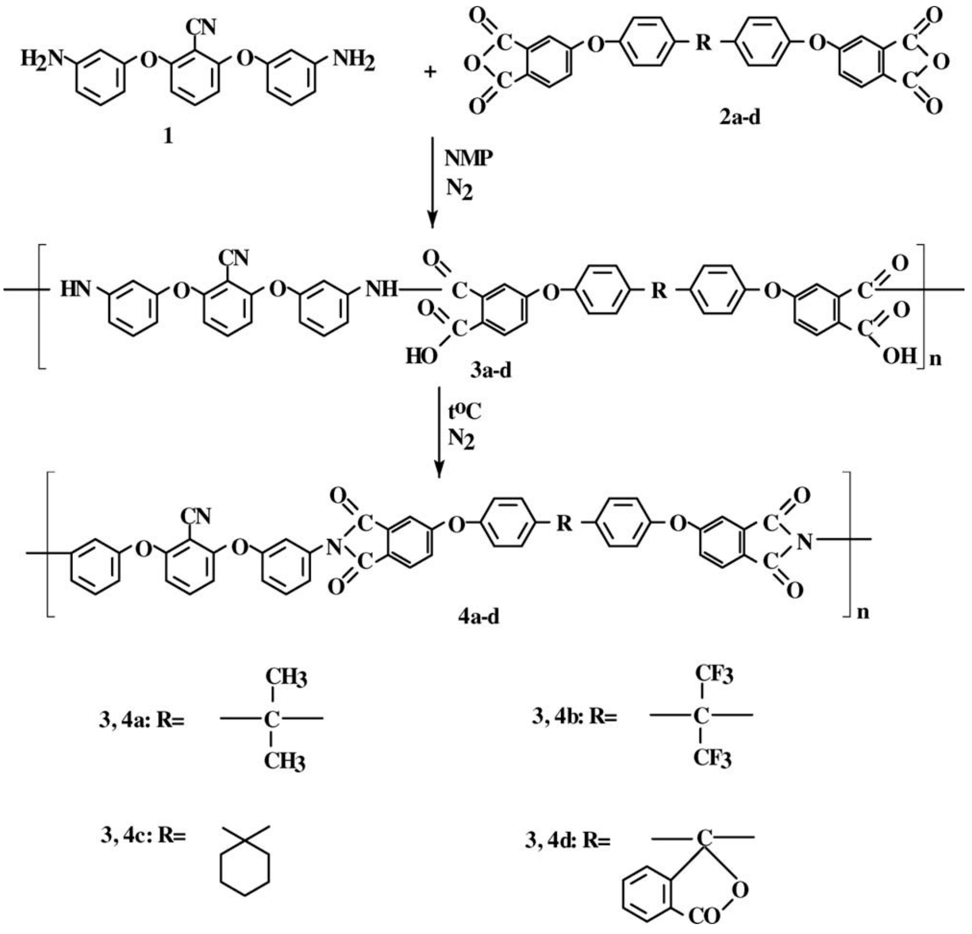

Scheme 1 Synthesis of polymers **3** and **4**.

acetic anhydride. m.p.**2a** = 189–190°C, m.p.**2b** = 229–231°C, m.p.**2c** = 195–197°C, and m.p.**2d** = 191–193°C.

Poly(ether imide)s **4** were synthesized by a two-step polycondensation reaction of 2,6-bis-(*m*-aminophenoxy)benzonitrile (**1**) with 2,2-bis[4-(3,4-dicarboxyphenoxy)phenyl] isopropane dianhydride (**2a**), 2,2-bis[4-(3,4-dicarboxyphenoxy)phenyl]hexafluoroisopropane dianhydride (**2b**), 1,1-bis[4-(3,4-dicarboxyphenoxy)phenyl]cyclohexane dianhydride (**2c**), or 3,3-bis[4-(3,4-dicarboxyphenoxy)phenyl]phthalide dianhydride (**2d**), respectively. The reactions were run with equimolar quantities of monomers, at a concentration of 12–15% total solids, in *N*-methylpyrrolidinone as solvent. In the first step, the polyamidic acid **3** was obtained. The reaction was run at room temperature and constant stirring, under a stream of nitrogen.[23] In the second step, the polyamidic acid was converted into the corresponding poly(ether imide) **4** by cyclodehydration at high temperature (180–190°C); a slow stream of nitrogen was used to remove the water formed during the imidization process (Scheme 1). The total yield was of 96%. The results of nitrogen content from elemental analyses for polymers **4** were: **4a** ($C_{50}H_{28}N_3O_8$), calcd: 5.26%, found: 5.18%; **4b** ($C_{50}H_{25}N_3F_6O_8$), calcd: 4.62%, found: 4.58%; **4c** ($C_{53}H_{35}N_3O_8$), calcd: 4.99%, found: 4.87%; **4d** ($C_{55}H_{29}N_3O_{10}$), calcd: 4.71%, found: 4.64%.

Preparation of thin polymer films

To obtain films of poly(ether imide)s **4**, polymer solutions of 12% concentration in NMP were cast onto glass plates and were gradually heated from room temperature up to 220°C, and the heating was continued for an additional 1 h. The resulting films showed a strong adhesion to the glass support and were stripped off the plates by immersion in water, followed by drying in oven at 110°C. These films had the thickness in the range of 30–80 μm and were used afterward for various measurements. To perform the crosslinking study, the films as-deposited on glass plates were cured by heating up to 400°C and kept at 400°C for 5 h. The cured films were stripped off the plates by immersion in boiling water, followed by drying in oven at 110°C.

Diluted polymer solutions in NMP with concentration of 1% were spin-coated onto silicon wafers at a speed of 5000 rpm to obtain very thin films having

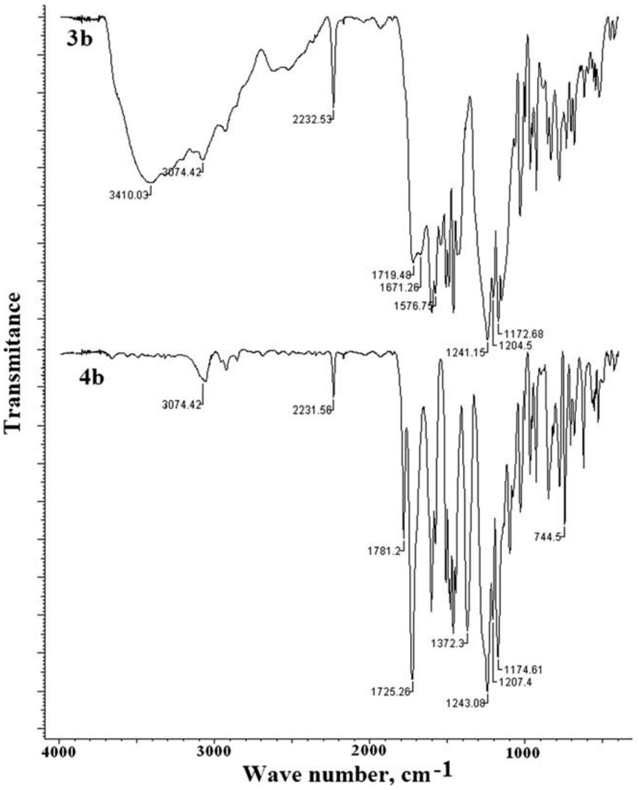

Figure 1 FTIR spectra of the polyamidic acid **3b** and of the corresponding poly(ether imide) **4b**.

the thickness in the range of nanometers. These films, as-deposited, were gradually heated up to 200°C in the same way as described earlier to remove the solvent and were used afterward for AFM investigations.

RESULTS AND DISSCUSION

General characterization

The structural identification of the polymers was made by elemental analyses, Fourier Transform Infrared (FTIR) and H^1-NMR spectroscopy.

The FTIR spectra of the polyamidic acid **3b** and of the corresponding poly(ether imide) **4b** confirm the structure of the polymers (Fig. 1). Thus, the two structures have common bands characteristic for the hexafluoroisopropylidene unit at 1210 and 1170 cm^{-1}, the band for the nitrile group at 2230 cm^{-1}, the band for C–H linkage at 3070 cm^{-1}, and the band for the aromatic ether linkage at 1240 cm^{-1}. The FTIR spectrum of polymer **3b** shows the absorption band characteristic for carboxylic group at 3410 cm^{-1}, and for the amidic unit at 1671 and 1576 cm^{-1}. The cyclization of the intermediate product **3b** to the corresponding imide structure **4b** was confirmed by the disappearance of these bands and by the presence of absorption bands characteristic to imide groups at 1781 and 1720 cm^{-1} due to the vibration of the asymmetric and symmetric of C=O unit, at 1372 cm^{-1} due to the vibration of the C–N stretching and at 744 cm^{-1} due to the vibration of the imide ring. The FTIR spectra of poly(ether imide)s **4a** and **4c** show the characteristic band for C–H aliphatic group at 2970 cm^{-1}.

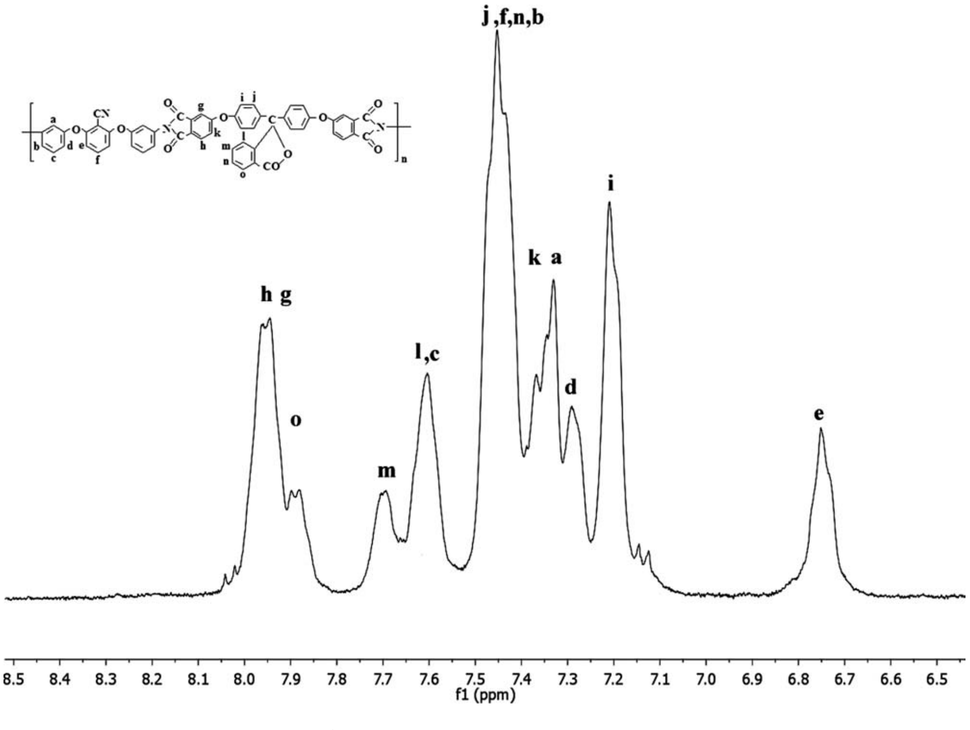

Figure 2 H^1-NMR spectrum of poly(ether imide) **4d**.

TABLE I
Solubility of Poly(ether imide)s 4

Polymer	Solvent						
	$CHCl_3$	CH_2Cl_2	THF	Acetone	DMSO	DMAc	NMP
4a	++	++	++	−	++	++	++
4b	++	++	++	−	++	++	++
4c	++	++	++	−	++	++	++
4d	++	++	+−	−	++	++	++

$CHCl_3$, chloroform; CH_2Cl_2, methylene choride; THF, tetrahydrofurane; DMSO, dimethylsulfoxide; DMAc, *N*,*N*-dimethylacetamide; NMP, *N*-methylpyrolidinone.

++ soluble at room temperature; +− partially soluble; − insoluble even at heating.

The conversion of the poly(amic acid)s to the corresponding poly(ether imide) structures was also confirmed by the fact that ^{1}H-NMR spectra of polymers **4** showed no residual resonance in the region 9–11 ppm indicating the absence of amide NH protons. Figure 2 shows H^1-NMR spectrum of poly (ether imide) **4d**, as an example, with the assignment for all the protons.

These poly(ether imide)s are soluble in organic solvents such as *N*-methylpyrollidinone, *N*,*N*-dimethylacetamide, and dimethylsulfoxide, as well as in less polar solvents such as tetrahydrofurane, chloroform, and methylene chloride (Table I). Poly(ether imide) **4d** is only partially soluble in THF, probably due to the presence of rigid phthalide group.

The improved solubility of these polymers, compared with wholly aromatic polyimides which are totally insoluble in organic solvents, can be explained by the introduction in the structural unit of the flexible ether bridges, present in both monomers, which do not allow a tight packing of the macromolecular chains. Figure 3 shows the molecular model of poly (ether imide) **4d** from which it can be noticed that the shape of the polymer is far from the rigid-rod one characteristic for conventional polyimides.

Inherent viscosities and molecular weights for polymers **4** are presented in Table II.

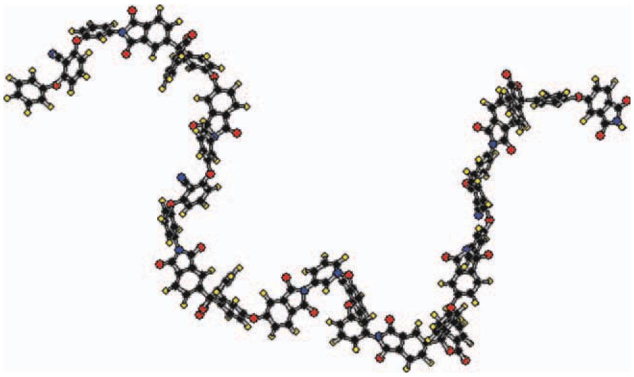

Figure 3 Molecular model of a fragment incorporating 4 structural units of poly(ether imide) **4d**. [Color figure can be viewed in the online issue, which is available at wileyonlinelibrary.com.]

The crystallinity of the poly(ether imide)s was examined by WAXD. The diffraction patterns were broad with no well-defined peaks (Fig. 4).

The studied polymers have the ability of forming thin, flexible, and transparent films by casting technique. The quality of very thin films prepared from dilute solutions of polymers at a concentration of 1% in NMP was investigated by AFM measurements which showed that the surface of the films was smooth, without pinholes or defects. Figure 5(a) presents the bidimensional image and Figure 4(b) the tridimensional image of poly(ether imide) **4d**. The root mean square roughness over an area of 5 × 5 μm^2 was of 0.46 nm.

Thermal properties

The thermal stability of the polymers was investigated by differential scanning calorimetry (DSC) and thermogravimetric analyses (TGA).

The glass transition temperature (T_g), determined by DSC, has the values in the range of 187–232°C (Fig. 6). The polymer containing flexible isopropylidene units (**4a**) has the lowest value of T_g (187°C), while poly(ether imide) **4d** containing rigid phthalide units has the highest value (232°C) of T_g, respectively.

The thermogravimetric (TG) and derivative thermogravimetric (DTG) curves for polymers **4** at a heating rate of 10°C min^{-1} are presented in Figure 7.

The main thermogravimetric data at four heating rates of poly(ether imide)s **4** are presented in Table III.

TABLE II
Inherent Viscosity and Molecular Weights of Polymers 4

Polymer	η_{inh}[a] (dL/g)	*Mn* (g/mol)	*Mw* (g/mol)	*Mw/Mn*
4a	0.53	9812	17,100	1.743
4b	0.61	10,899	17,997	1.651
4c	0.38	6286	9362	1.489
4d	0.42	7425	10,561	1.422

[a] Measured at a concentration of 0.5 g polymer in 100 mL of NMP, at 20°C.

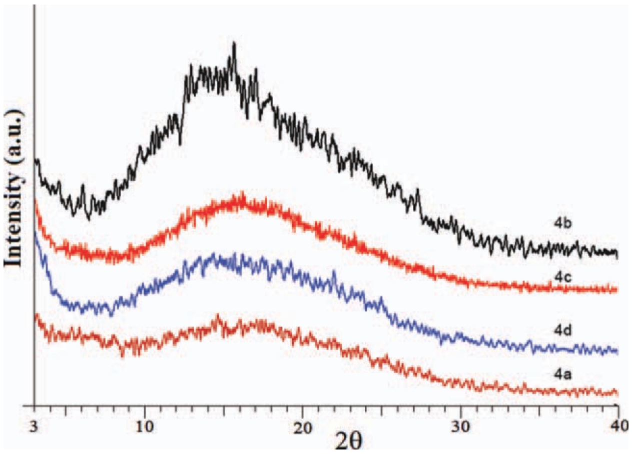

Figure 4 WAXD diffraction patterns at room temperature of polymers **4**. [Color figure can be viewed in the online issue, which is available at wileyonlinelibrary.com.]

All the polymers have a good thermal stability, with initial decomposition temperature beeing above 400°C for all four heating rates. The degradation process takes place in two stages, with different weight losses depending on the chemical structures of the polymers.

The degradation mechanism does not change with the increase of the heating rate, the shape of TG and DTG curves being the same (Fig. 8).

If we consider the temperature corresponding to the start of decomposition (T_{onset}) as a criterion of thermal stability, we obtain the following series of thermostabilities:

4**d** < 4**c** < 4**b** < 4**a**

Another criterion of the thermal stability is the temperature of maximum decomposition speed of the first stage ($T_{peak\ 1}$). Based on this criterion, the series of thermostabilities changes, so that a reverse in the thermostability of samples **4b** and **4a** appears: the speed of decomposition of polymer **4a** is much higher than that of the polymer **4b** in the first stage, considering the temperature range in which this process takes place.

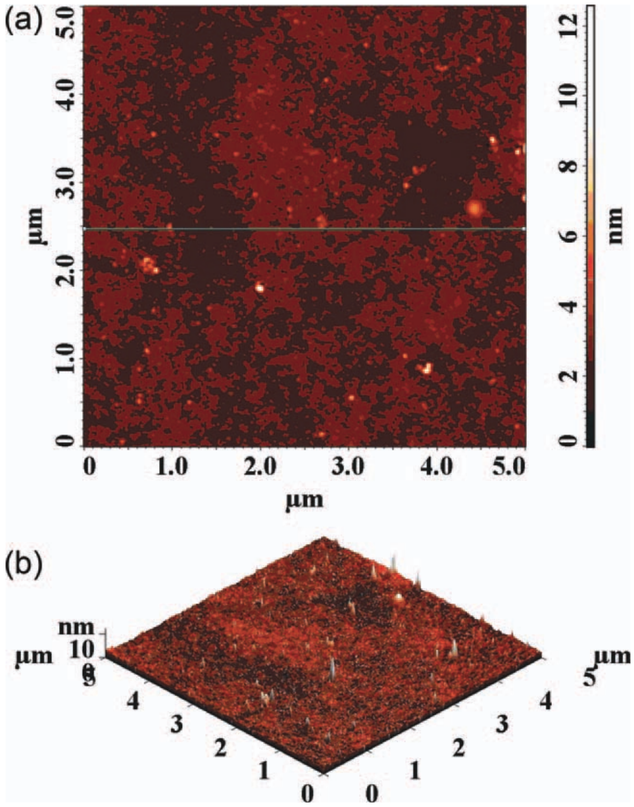

Figure 5 AFM image of poly(ether imide) **4d**: (a) 2D-image; (b) 3D-image. [Color figure can be viewed in the online issue, which is available at wileyonlinelibrary.com.]

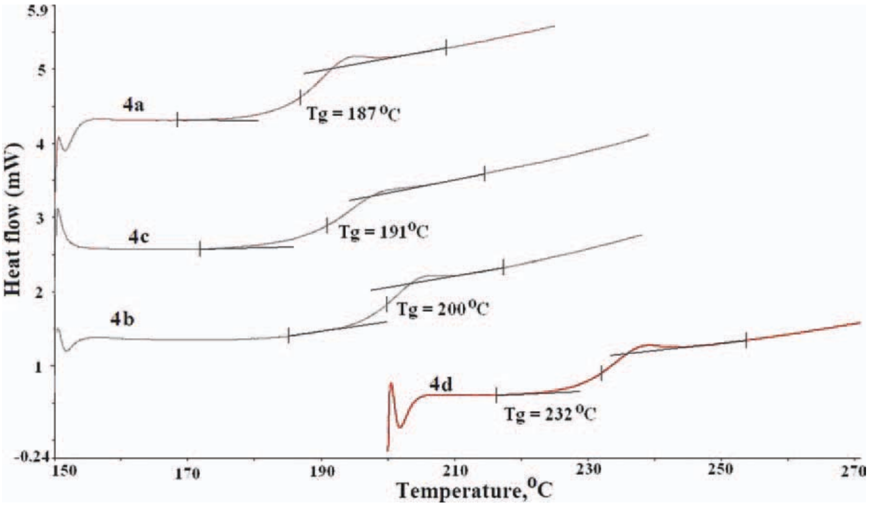

Figure 6 DSC curves of poly(ether imide)s **4**. [Color figure can be viewed in the online issue, which is available at wileyonlinelibrary.com.]

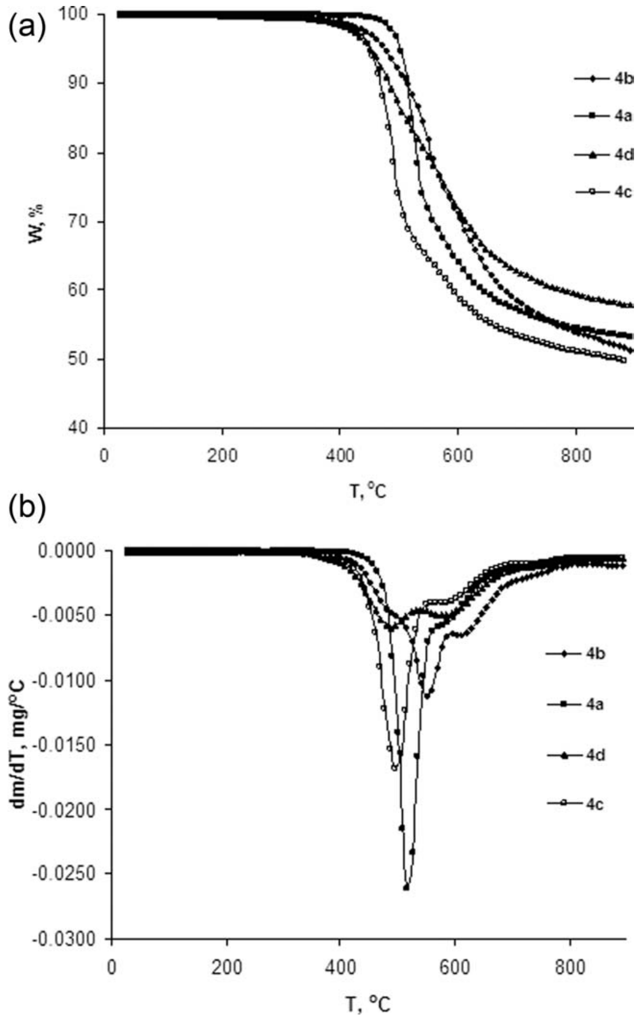

Figure 7 TG and DTG curves for polymers **4** at a heating rate of 10°C min^{-1}: (a) TG curves and (b) DTG curves.

4**d** < 4**c** < 4**a** < 4**b**

A kinetic study was performed by using the thermogravimetric parameters. At maximum speed of decomposition, ASTM E-698 standard method was applied, which uses the eq. (1) for the calculation of activation energy:[24]

$$\ln \frac{a}{T_{\text{peak}}^2} = \ln \frac{\text{AR}}{E_a} - \frac{E_a}{R} \cdot \frac{1}{T_{\text{peak}}} \tag{1}$$

where a represents the heating rate (7, 10, 13, and 16°C min^{-1}), R is the gas contant, E_a is the activation energy, A is the pre-exponential factor, and T_{peak} is the temperature of maximum decomposition speed. The kinetic parameters obtained by using this method are listed in Table IV.

The results obtained for the activation energy confirm the fact that polymer **4b** has the highest thermostability, when the speed of degradation of the polymers is taken as a criterion of thermostability. To obtain the activation energy at different degrees of conversion, ASTM–E1641 standard method was applied using eq. (2):[25]

$$\log a = \log \frac{A \cdot E_a}{R} - \log F(\alpha) - 2.315 - 0.4567 \frac{E_a}{\text{RT}} \tag{2}$$

where $F(\alpha)$ is the conversion function. The value of E_a when α = constant can be determined from the intercept slope obtained from the log $a = f(1/T)$ plot (Fig. 9).

The results show that the thermal decomposition process is complex because the activation energy varies with the conversion degree. For polymers **4b** and **4d**, the activation energy increases with the increase of conversion degree; it has a maximum, then it decreases and, at higher values of conversion degree, one or two maxima of the activation energy appear. For polymers **4a** and **4c**, at conversion degrees between 10 and 50%, the activation energy has approximately constant values; at 70% conversion degree, a maximum of activation energy is observed. The values of activation energy, at low conversion degrees, confirm the thermostability series previously established from thermal data (criterion on T_{onset}).

Molecular relaxations

Generally, amorphous polymers have, at high temperature, a primary relaxation, α, which is assigned to the glass transition temperature; at low and moderate temperature, at least two secondary relaxation processes, γ and β are shown.[26]

Figure 10 shows the temperature dependence of storage modulus (E'), loss modulus (E'') and mechanical loss tangent (*tan* δ) for poly(ether imide) **4a**, before crosslinking. The drops in E' curves and the peaks in E'' and *tan* δ plots indicate the physical transitions which take place in the macromolecules. At very low temperatures, the polymers exhibit a plateau above 10^9 Pa, a region where the macromolecules are in the "frozen" state which is typical for glassy polymers.

As it can be seen on the E'' curve, at low temperature of about −90°C, a secondary γ relaxation appears due to the phenyl ring motions, and it is influenced by the moisture absorption content, aging history, and morphology.[27,28] At higher values of temperature, of about 30°C, the β relaxation process can be noticed which is attributed to the noncooperative motions of the phenylene groups from the diamine or the dianhydride units, around flexible linkages such as –O–, –CH_2–, etc.[29] The broadness of this relaxation is due to the high values of relaxation times which characterize a heterogenic structure. At

TABLE III
Thermogravimetric Parameters for Poly(ether imide)s 4

Polymer	Heating rate (°C/min)	Stage	T_{onset} (°C)	T_{peak} (°C)	T_{endset} (°C)	W%	Residue (900°C)
4a	7	I	484	516	536	27.41	50.50
		II	536	590	732	22.09	
	10	I	490	525	542	27.79	52.54
		II	542	598	666	19.67	
	13	I	500	531	560	29.81	50.89
		II	560	615	773	19.30	
	16	I	499	536	559	27.00	51.94
		II	559	611	791	21.06	
4b	7	I	447	547	559	20.57	54.80
		II	559	607	776	24.63	
	10	I	455	551	570	24.67	51.15
		II	570	613	767	24.18	
	13	I	455	558	574	21.86	52.65
		II	574	624	753	25.49	
	16	I	458	561	582	21.66	55.00
		II	582	626	796	23.34	
4c	7	I	440	489	514	31.33	48.67
		II	514	588	690	20.00	
	10	I	455	497	526	31.31	48.00
		II	526	593	668	20.69	
	13	I	462	504	529	29.52	49.75
		II	529	602	750	20.73	
	16	I	463	509	536	30.17	48.36
		II	536	605	677	21.47	
4d	7	I	410	477	541	18.91	57.27
		II	541	578	742	23.82	
	10	I	433	487	560	22.05	57.79
		II	560	588	764	20.16	
	13	I	441	494	528	19.13	56.76
		II	528	589	786	24.11	
	16	I	443	501	537	19.12	56.82
		II	537	592	805	24.06	

T_{onset}, initial decomposition temperature; T_{peak}, temperature of maximum decomposition; T_{endset}, temperature of which the degradation process of each process ends, W%, weight loss at the corresponding stage of decomposition, %.

very high temperature, of about 200°C, the primary relaxation α is evidenced which is influenced by the rigidity of the macromolecular chains. In this region, the chains begin to coordinate large scale motions. One classical description is that the amorphous regions have begun to melt. The raise of the temperature induces motions of the whole polymer chain, and the slippage of the chains past each other can take place, and as result, the experiment cannot be conducted over 230°C.

To analyze the influence of frequency on the viscoelastic parameters E', E'', and *tan* δ, a DMA experiment at various frequencies of 0.5, 1, 2, 5, and 10 Hz was performed. As can be seen from Figure 11, the glass transition moves to higher values of temperature as the frequency increases. When the applied stress is faster, the macromolecules have less time to respond, and thus, a higher temperature is needed to stimulate the coordinated long range movements, characteristic for glass transition.[30]

To demonstrate that the relaxation from 200°C can be assigned to glass transition temperature, the activation energy was calculated using Arrhenius equation (3):

$$f = A\,exp(-E_a/RT) \tag{3}$$

where f is the frequency, A is the pre-exponential factor, E_a is the activation energy, R is the gas constant, and T is the absolute peak temperature. To use this equation for the cooperative processes, it is necessary to apply the relation within a narrow range of frequencies. The activation energy calculated from Arrhenius plot is 840.74 kJ mol^{-1}, with a linear relative coefficient of 0.995 corresponding to a α-relaxation.

DEA and DMA are used to evidence the secondary and primary transitions which take place in the polymers structure. DEA also allows the calculation of activation energy characteristic to these processes

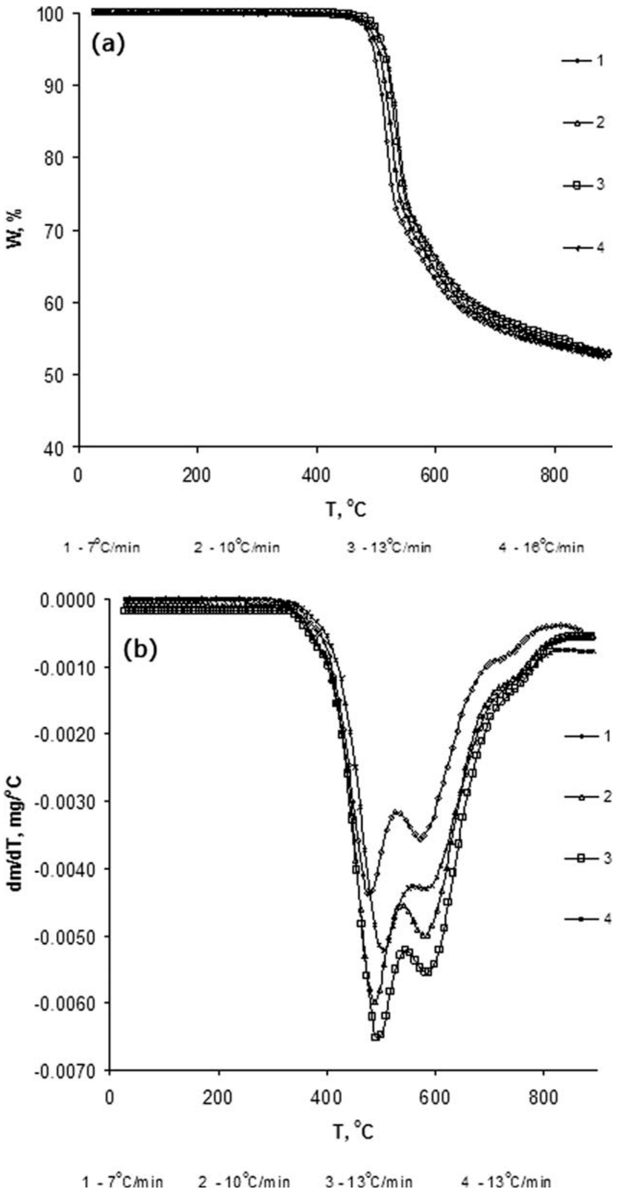

Figure 8 TG and DTG curves for polymers **4** at different heating rate: (a) TG curves and (b) DTG curves.

with the aim to demonstrate the nature of the relaxations. Figure 12 shows the dependence of dielectric loss (ε″) over a large domain of temperature and frequency for poly(ether imide) **4a**. It can be noticed that at low values of temperature, the γ transition appears. With the temperature increase, the β relaxation appears. Its shape is similar to that obtained from the DMA curves having a broad distribution. The α relaxation can be identified at higher temperatures, of about 200°C, in the same region as the one identified from DMA analysis.

TABLE IV
The Values of Kinetic Parameters Calculated with the ASTM E-698 Standard Method

Polymer	n[a]	E_a (kJ/mol)[b]	ln A[c]	r^2[d]
4a	1	185.87	22.87	0.999
4b	1	256.99	32.54	0.997
4c	1	200.34	26.26	0.997
4d	1	122.85	14.13	0.998

[a] Reaction order.
[b] Activation energy.
[c] Pre-exponential factor.
[d] Correlation coefficient.

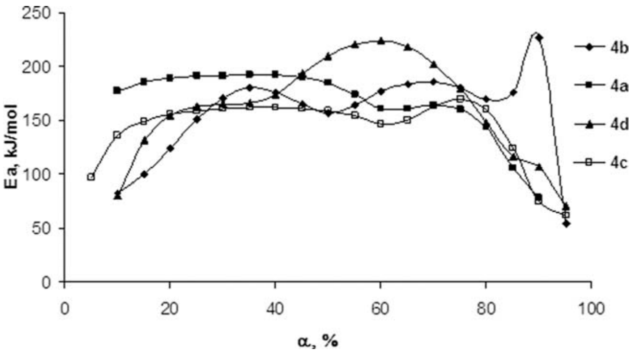

Figure 9 Variation of activation energy with conversion degree.

With the increase of frequency, the maximum peak of relaxations moves to higher values of temperature. It can be noticed that DEA evidenced the same transitions as DMA.

The activation energy was calculated using Arrhenius equation (3). The E_a value for γ transition was 40.79 kJ mol^{-1} and for β was 103.35 kJ mol^{-1}, which corresponds to secondary relaxations.

Polymer crosslinking

The modification in the value of glass transition trempérature (T_g) is used to monitor the changes that occur in the polymer chains, such as plasticizing due

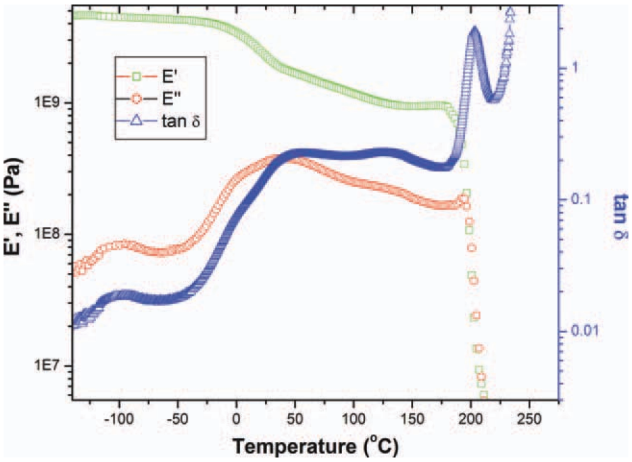

Figure 10 Temperature dependence of the storage modulus (E'), loss modulus (E'') and mechanical loss tangent (*tan* δ) for poly(ether imide) **4a**, before crosslinking. [Color figure can be viewed in the online issue, which is available at wileyonlinelibrary.com.]

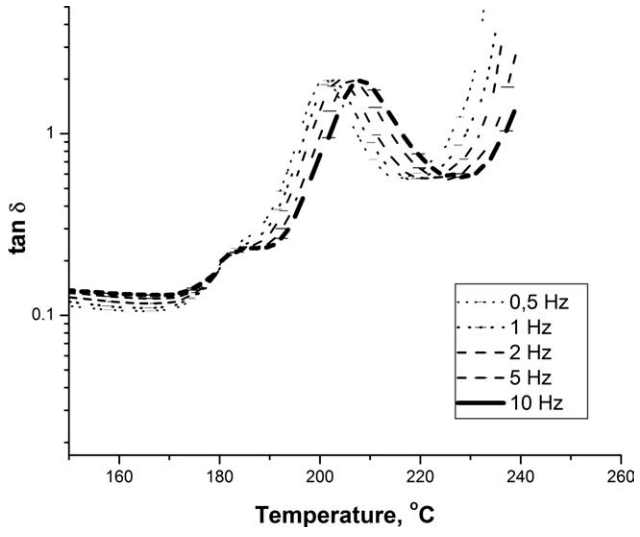

Figure 11 The *tan* δ behavior of poly(ether imide) **4a** at different frequencies.

to the environmental solvents and to the crosslinking caused by thermal or ultraviolet aging. For thermosetting resins, it cannot be detected any process after glass transition, unless the material burns and degrades, because the crosslinking impedes the slippage of the chains past each other. The glass transition temperature of cured materials or thin coatings is difficult to evaluate. DMA is the most appropriate method for this measure because it is 10 to 100 times more sensitive at T_g changes than DSC or DTA. The glass transition temperature of highly crosslinked materials can easily be seen long after the T_g becomes too flat and broad to be detected in DSC.[31]

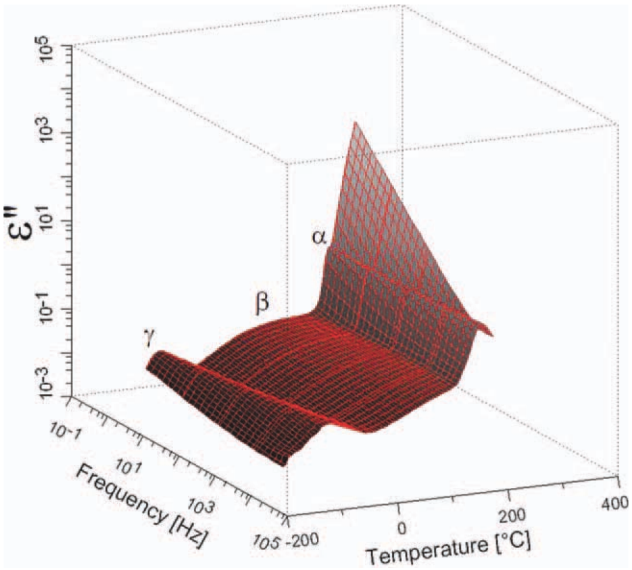

Figure 12 Dependence of dielectric loss (ε″) on temperature and frequency for poly(ether imide) **4a**. [Color figure can be viewed in the online issue, which is available at wileyonlinelibrary.com.]

Poly(ether imide) films, made from solutions of 12% concentration in NMP, were thermally treated up to 400°C to promote the crosslinking of CN groups to insoluble products probably due to the formation of *s*-triazine rings, according to the literature.[10,32] The crosslinking of the polymer films after thermal treatment was evidenced by DMA and DSC analyses, solubility measurements. and FTIR spectroscopy.

Figure 13 shows the temperature dependence of the storage modulus (E'), loss modulus (E''), and mechanical loss tangent (*tan* δ) for poly(ether imide) **4a**, after crosslinking. Thus, at low temperature of −95°C, the γ transition can be noticed. The β transition has some significant differences in the broadness and value of temperature: the peak is narrower and its temperature is found to be approximately at 50°C, a little higher than that corresponding to the original film (30°C). The flattening of the β transition curve, which is influenced by the motions of the phenylene groups around flexible linkages, suggests that the structure has a higher rigidity due to the existence of some crosslinkings along the chains. The free volume of the film is not able to expand with the increase of temperature because of the crosslinking, and thus, the glass transition temperature does not have the same intensity, being almost undetectable.

DSC curves did not evidence a glass transition temperature of the cured polymer films.

Another method used to demonstrate the existence of *s*-triazine is solubility measurement. The insolubility of cured poly(ether imide) films in organic solvents, such as NMP, DMF, and DMSO, demonstrates the appearance of tridimensional networks between the macromolecular chains, which

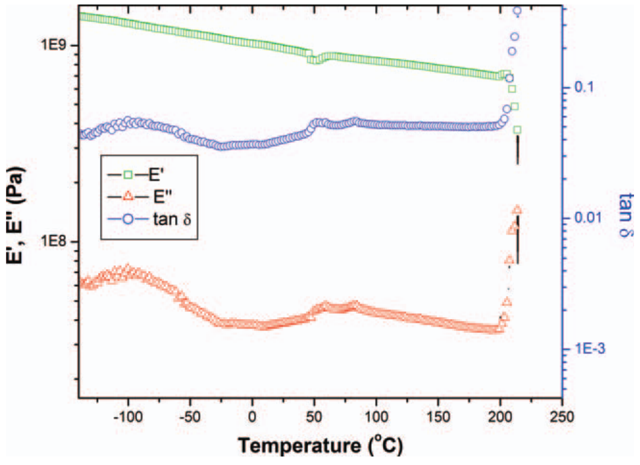

Figure 13 Temperature dependence of the storage modulus (E'), loss modulus (E'') and mechanical loss tangent (*tan* δ) for poly(ether imide) **4a**, after crosslinking. [Color figure can be viewed in the online issue, which is available at wileyonlinelibrary.com.]

give a higher rigidity of the cured polymers. Thus, the small molecules of solvent cannot penetrate through the chains to realize the dissolution of the polymers. The insolubility of polymers after curing at high temperature is very important from a practical point of view in the way that the polymer films would maintain they shape at high temperature and would be completely resistant to organic solvents.[33]

FTIR spectra of the treated polymer films are not concludent in identification of *s*-triazine because the characteristic band of absorbtion for C=C aromatic linkage found at 1500 cm^{-1} overlaps the one due to the new C=N group at 1495 cm^{-1} formed by crosslinking.

CONCLUSIONS

Poly(ether imide)s **4** were synthesized by polycondensation reaction of different bis(ether dianhydride)s containing isopropylidene, hexafluoroisopropylidene, cyclohexane, and phthalide units with 2,6-bis(*m*-aminophenoxy)benzonitrile. These polymers are soluble in polar aprotic solvents such as *N*-methylpyrollidinone, *N*,*N*-dimethylacetamide, and dimethylsulfoxide and in less polar solvents such as tetrahydrofurane, chloroform, and methylene chloride, having improved solubility compared with conventional wholly aromatic polyimides. These polymers can be easily processed into thin films by casting their solutions. The films are smooth, homogenous, and free of defects.

The polymers have a good thermal stability, with initial decomposition temperature being above 400°C independent on the heating rate. The high thermal stability is also confirmed by the high values of activation energies of decomposition.

The glass transition temperature of the studied poly(ether imide)s is situated in the range of 187–232°C; the polymer **4a** containing isopropylidene units has the smallest value, while the polymer **4d** which incorporates pendant phthalide groups has the highest value.

DMA evidenced the primary and secondary transitions which took place in the macromolecules and allowed the calculation of the activation energy for α transition using a narrow range of frequency. The crosslinking of the nitrile group to *s*-triazine rings was demonstrated by the flattening of β transition curve and by the disappearance of glass transition temperature in DMA curves. The insolubility of the cured films in organic solvents, compared with the solubility of the uncured samples, evidenced the presence of tridimensional networks as a result of crosslinking.

DEA measurements also evidenced the molecular relaxations in the polymer chains. The values calculated for activation energy of 40.79 kJ mol^{-1} and 103.35 kJ mol^{-1}, respectively, demonstrate the secondary transitions γ and β.

References

1. Hergenrother, P. M. High Perform Polym 2003, 15, 3.
2. Hamciuc, C.; Hamciuc, E.; Ipate, A. M.; Okrasa, L. Polymer 2008, 49, 681.
3. Damaceanu, M. D.; Bacosca, I.; Bruma, M.; Robison, J.; Rusanov, A. L. Polym Int 2009, 58, 1041.
4. Hamciuc, E.; Hamciuc, C.; Bacosca, I.; Olariu, M. Mater Plast 2010, 47, 11.
5. Taguchi, Y.; Uyama, H.; Kobayashi, S. J Polym Sci Part A: Polym Chem 1997, 35, 271.
6. Keller, T. M. J Polym Sci Part A: Polym Chem 1987, 25, 2569.
7. Lee, Y. J.; Lee, E. M.; Lee, M. H.; Oh, M. C.; Ahn, J. H.; Han, S. G. J Polym Sci Part A: Polym Chem 1998, 36, 2881.
8. Haddad, I.; Hurley, S.; Marvel, C. S. J Polym Sci Part A: Polym Chem 1973, 11, 261.
9. Keller, T. M.; Dominguez, D. D. Polymer 2005, 46, 4164.
10. Bruma, M.; Mercer, F.; Schulz, B.; Dietel, R.; Fitch, J.; Cassidy, P. High Perform Polym 1994, 6, 183.
11. Hsu, L. C. Pat. Appl. 4,555,565 (1985).
12. Park, C.; Ounaies, Z.; Wise, K. E.; Harrison, J. S. Polymer 2004, 45, 5417.
13. Gonzalo, B.; Vilas, J. L.; Breczewski, T.; Perez-Jubindo, M. A.; de la Fuente, M. R.; Rodriguez, M.; Leon, L. M. J Polym Sci Part A: Polym Chem 2009, 47, 722.
14. Hamciuc, E.; Hamciuc, C.; Bacosca, I. Rev Roum Chim 2010, 55, 515.
15. Hamciuc, C.; Hamciuc, E.; Ignat, M.; Zarnescu, G. High Perform Polym 2009, 21, 205.
16. Hypercube Inc. (Ontario), Hyperchem, 2002, Version 7.5.
17. Hearth, D. R.; Wirth, J. G. U.S. Pat. 3,763,211 (1973).
18. Bacosca, I.; Hamciuc, E.; Bruma, M.; Ronova, I. A. High Perform Polym 2010, 22, 703.
19. Heath, D. R.; Wirth, J. G. U.S. Pat. 3,956,320 (1976).
20. Schwartz, W. T., Jr. High Perform Polym 1990, 2, 189.
21. Yang, C. P.; Yu, C. W. J Polym Sci Part A: Polym Chem 2001, 39, 788.
22. Yang, C. P.; Su, Y. Y. J Polym Sci Part A: Polym Chem 2006, 44, 3140.
23. Sroog, C. E. J Polym Sci Part C: Polym Lett 1991, 16, 561.
24. ASTM Test Method E698. Standard Test Method for Arrhenius Kinetic Constants for Thermally Unstable Materials, ASTM International, West Conshohocken, PA, 1984, p 56.
25. ASTM Test Method E1641. Standard Test Method for Decomposition Kinetics by Thermogravimetry, ASTM Book of Standards 14.02, American Society for Testing and Materials, 1994, p 1042.
26. Bas, C.; Tamagna, C.; Pascal, T.; Alberola, N. D. Polym Eng Sci 2003, 43, 344.
27. Habas, J. P.; Peyrelasse, J.; Grenier-Loustalot, M. F. High Perform Polym 1996, 8, 515.
28. Jonas, A.; Legras, R. Macromolecules 1993, 26, 813.
29. Wenli, Q.; Ko, T. M.; Vora, R. H.; Chung, T. S. Polymer 2001, 42, 6393.
30. Cristea, M.; Gheorghiu Ionita, D.; Bruma, M.; Simionescu, B. C. J Therm Anal Calorim 2008, 93, 63.
31. Menard, K. V. Dynamic Mechanical Analysis; CRC Press: Boca Raton, 1999.
32. Saxena, A; Prabhakaran, P. V.; Rao, V. L.; Ninan, K. N. Polym Int 2005, 54, 544.
33. Bruma, M.; Schulz, B.; Kopnick, T.; Dietel, R.; Stiller, B.; Mercer, F.; Reddy, V. N. High Perform Polym 1998, 10, 207.